

키토산과 대나무 숯/실리카 혼성체가 보강된 스티렌-부타디엔 고무복합체의 연구

리시양수* · 조을룡***† 

*한국기술교육대학교 에너지, 신소재, 화학공학부, **친환경고성능화학소재연구소
(2018년 4월 9일 접수, 2018년 6월 20일 수정, 2018년 6월 20일 채택)

Study on Styrene-Butadiene Rubber Composites Reinforced by Hybrids of Chitosan and Bamboo Charcoal/Silica

Xiang Xu Li* and Ur Ryong Cho***† 

*School of Energy, Materials and Chemical Engineering, Korea University of Technology and Education, Cheonan, Chungnam 31253, Korea

**Research Center of Eco-friendly & High-performance Chemical Materials, Cheonan, Chungnam 31253, Korea

(Received April 9, 2018; Revised June 20, 2018; Accepted June 20, 2018)

초록: 키토산-폴리(비닐 알코올)(CS-PVA) 젤 및 충전제[땀부차콜(BC) 및 실리카(SI)] 첨가에 대한 스티렌-부타디엔 고무의 점탄성 물성을 조사하였다. 스티렌-부타디엔 고무 라텍스에 상호 침투 가교 방법으로 제조된 키토산-PVA-땀부차콜/실리카(BC/SI-CS-PVA) 혼성체를 혼합하여 고무복합체를 제조하였다. 고무 가공분석기의 변형 스위프(strain sweep) 및 주파수 스위프(frequency sweep) 기능을 사용하여 제조된 복합체(composites) 및 가황체(vulcanizates)의 점탄성을 조사하였다. 주사전자현미경 및 내마모성 측정을 통해서 가교 구성 및 기계적 물성을 확인하였다. 충전제의 종류에 따라서 스티렌-부타디엔 고무의 저장 탄성률(G') 및 탄성 토크(S')는 현저하게 증가하였다. 실험 결과를 통해서 BC-CS-PVA 혼성체가 가장 높은 저장 탄성률(G'), 탄성 토크(S') 및 내마모성의 결과를 보였다. 따라서 BC-CS-PVA 혼성체가 SBR 복합체에 가장 좋은 점탄성 물성 및 기계적 물성의 보강 효과를 보였다.

Abstract: The influences of chitosan-poly(vinyl alcohol) (CS-PVA) gel and different fillers [bamboo charcoal (BC) and silica (SI)] on the viscoelastic properties of styrene-butadiene rubber (SBR) were studied in this work. The chitosan-PVA-bamboo charcoal/silica (BC/SI-CS-PVA) hybrid fillers compatibilized SBR composites were fabricated by interpenetrating polymer network (IPN) method. The viscoelastic behaviors of the rubber composites and their vulcanizates were explored using a rubber processing analyzer (RPA) in the modes of strain and frequency sweeps. Storage modulus (G') and elastic torque (S') of the SBR increased significantly with the incorporation of different hybrid filler. BC-CS-PVA-SBR composite showed the highest storage modulus and elastic torque and abrasion resistance, which means BC-CS-PVA hybrid filler could make the best reinforcement of viscoelastic and mechanical properties for SBR material in this research.

Keywords: chitosan, bamboo charcoal, silica, gel, styrene butadiene rubber, viscoelastic properties.

Introduction

In recent years, bio-charcoal has been widely utilized as an alternative of carbon black in the research field of rubbery materials.¹ As a species of bio charcoal abundant in nature, bamboo charcoal (BC) has been proved a promising reinforcement in the fabrication of bio charcoal/polymer com-

posites. Its reinforcing effects on the macroscopic properties of rubber materials are mainly originated from the porous structure and larger specific surface.²

Recent research works about BC/rubber composites mainly focused on the modification of BC interface and uniform dispersion of BC in the matrixes. In the past few years, a great deal of synthesis strategies has been developed and applied in the preparation of BC polymer composite for the purpose mentioned above. But the effect of reinforcement always was not ideal.³

Chitosan (CS) also is a common biomaterial with many researches in recent years, but in rubbery filed, pure CS cannot

†To whom correspondence should be addressed.
urcho@koreatech.ac.kr, ORCID  0000-0003-4866-8109
©2018 The Polymer Society of Korea. All rights reserved.

provide any other reinforcement on mechanical properties due to its poor hydrophilicity which provide poor dispersion into rubber matrix. Li found that BC graft CS by synthesis sulfonated BC-CS hybrid could improve the mechanical properties with the carbon structure and the bio properties with the CS structure.⁴

And in the field of rubbery researches, the interpenetrating polymer network (IPN)⁵ and physical crosslinking had become hot issue in recent years. Almost physical crosslinking methods depend on noncovalent bond, such as hydrogen bond, van der Waals force and other intermolecular force.⁶ IPN is a polymer comprising two or more networks which are at least partially interlaced on a polymer scale but not covalently bonded to each other, which could provide more compact matrix structure.⁷ In IPN, when the physical crosslinking and chemical crosslinking occur simultaneously in a polymer material, it is speculated that the material may have better viscoelastic properties.

However, researches on the properties during the processing of IPN are far from sufficient, especially studies on the viscoelasticity of BC/CS rubber composites. The viscoelasticity of BC/CS rubber composites and their raw materials is of prime importance for the process ability and the performances of rubber products. Investigations on the relationships between modulus and dynamic strain amplitude or frequency are helpful for the understanding of macromolecule motions,⁸ crosslinking and filler-rubber interactions. This work is also meaningful in rubber industry which could be used as references for the fixing of processing parameters. And CS-PVA (poly(vinyl alcohol)) hydrogel system has good IPN structure, also exists physical crosslinking shown in Figure 1 and Figure 3, which could short the distance of rubber chain in latex state,⁹ and improve some properties of rubber matrix, so some researchers also pay their attention to this filed. Also, some researchers found formaldehyde or glutaraldehyde have been used as crosslink agent to crosslink CS and PVA which could make better IPN and provide better mechanical properties for the CS-PVA hydrogel (shown in Scheme 1, Scheme 2, Figure 2 and Figure 3),¹⁰ due to the adsorption force (hydrogen bonds) with filler particles, which also could increase the application of this material, such as the fillers.

In this research, styrene-butadiene rubber latex composites compatibilized with bamboo charcoal (BC)/silica (SI) CS PVA hybrids by IPN method reported previously, and neat SBR, BC-SBR and SI-SBR composites were also synthesized as control group. Various interactions between fillers and rubber

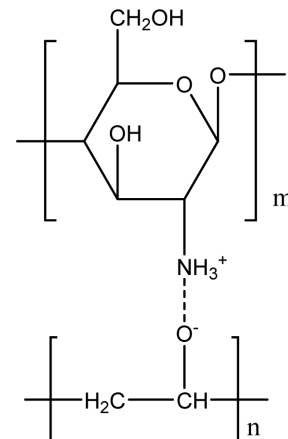
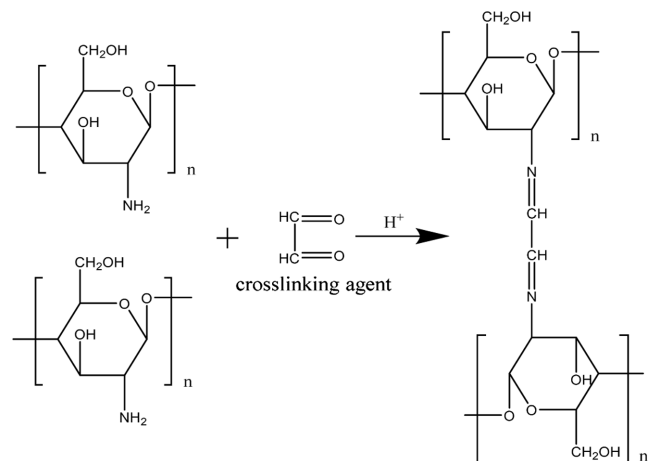
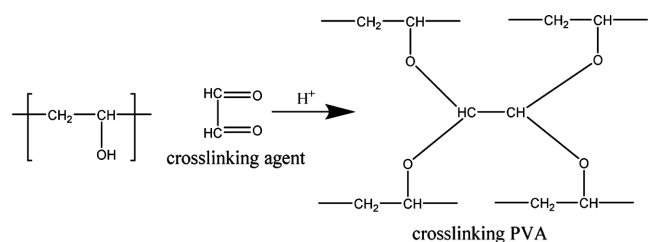


Figure 1. Hydrogen bond between chitosan and PVA.



Scheme 1. Synthesis of chitosan with formaldehyde crosslink agent.



Scheme 2. Synthesis of PVA with formaldehyde crosslink agent.

matrix were introduced by different hybrids, which led to various viscoelastic behaviors of the raw materials during strain amplitude sweep and frequency sweep. The viscoelastic behaviors were investigated in detail. Their relations with the interpenetrating structure with rubber chain and the other interactions between hybrid and matrix were explored, which are beneficial for better understanding of the filler-rubber system.

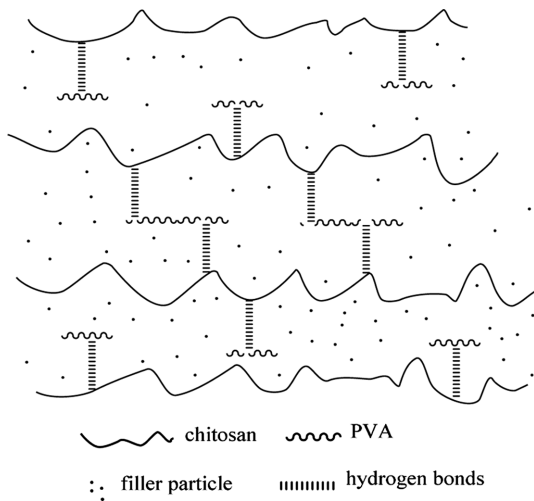


Figure 2. Formation mechanism of chitosan-PVA gel with filler.

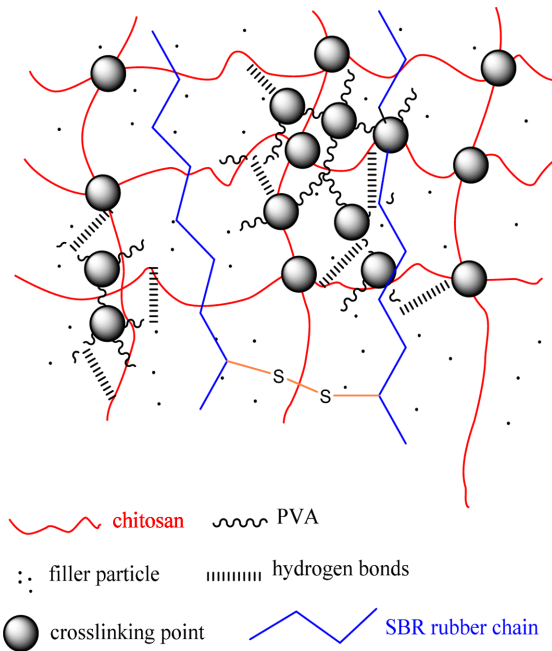


Figure 3. Formation mechanism of chitosan-PVA-filler interpenetrating gel with formaldehyde crosslink agent.

Experimental

Materials. Styrene-butadiene rubber latex 1502 (effective mass $61\pm 1\%$, styrene 23.5%) was obtained from Korea Kemho Petrochemical Company (KKPC), Korea; chitosan (CS) powder (microcrystalline) was obtained from DaeJung Company, Korea; bamboo charcoal (BC) powder was provided by Quzhou Minxin Charcoal Company, Zhejiang, China; silica (SI) was provided by Duksan Pure Chemical Company,

Korea; poly(vinyl alcohol) (PVA) 1500, extra pure (above 95%); sulfur, powder, extra pure (above 99%), and acetic acid, extra pure (above 99%) were purchased from Dae Jung Company, Korea; methanol, extra pure (99.5%); zinc oxide, extra pure (99%); stearic acid, extra pure (95%); dodecyl-benzene-sulfonic acid, sodium salt (DBS-Na) (50%); formaldehyde, extra pure (above 98%) were purchased from Samchun Pure Chemical Company, Korea; dodecyl sulfonate sodium (DBS-Na), extra pure (above 95%), was purchased from Dae Jung Company, Korea.

Synthesis for SI/BC-CS-PVA-SBR Composite. A 5 g amount of CS flakes was dissolved in 100 mL of dilute acetic acid (2% w/w) at 60 °C in a flask placed in a thermostatic water bath with a stirring speed of 148 rpm for 5 h. A 5 g amount of PVA was dissolved in 100 mL of deionized (DI) water in a beaker and agitated on a magnetic stirrer (at about 800 rpm) at 80 °C for 5 h.

The two solutions were then blended together with stirring on the magnetic stirrer (at about 800 rpm) at 70 °C for 48 h, after that, added 10 g SI or CS powder into the system and stirring at about 400 rpm and 60 °C for 2 h, then added about 2 g DBS-Na as the dispersion agent into SBR latex to improve the salting-out point of rubber latex.

After that, put the latex with DBS-Na into the gel system and stirring at room temperature for 2 h. Finally, dropped about 15 mL 25% formaldehyde aqueous solution into the system at 40 °C, then the products had been synthesized.

Compounding Process. The composites were dried in an oven at 70 °C until the weight kept constantly. The compounding process was conducted on a two roll mixing mill. And the formulation of conventional elastomeric additives was shown in Table 1.

Note the sulfur and accelerators were mixed in the final step to avoid the pre-vulcanization. Finally, the compounds were vulcanized under 10 MPa for t_{90} at 160 °C in a heat pressing machine (Auto hydraulic press type, Ocean Science). The thickness of the specimens was about 1 mm. For the purpose of comparison, we also prepared neat SBR, SBR filled with 10 phr SI and 10 phr BC.

Viscoelasticity of the Composites. In this part, the viscoelastic properties and the curing characteristic were determined with a rubber process analyzer (RPA-V1, U-Can Dynatex Inc., Taiwan). The morphology of the samples was carried out on a FE-SEM with EDS (JSM-7500F, JEOL Ltd. Japan). Abrasion resistance test was performed by Taber Abrasion tester 5135 according to ASTM D1044. There were

Table 1. Formulations of Test Sample Compounds

	Compositions									
	SBR ^c (phr)	Stearic acid (phr)	CBS ^a (phr)	DD ^b (phr)	Zinc oxide (phr)	Sulfur (phr)	Silica (phr)	Bamboo Charcoal (phr)	SI-CS- PVA-SBR (phr)	BC-CS- PVA-SBR (phr)
Neat SBR	100	2	2	0.5	3	1.75	0	0	0	0
SI-SBR	100	2	2	0.5	3	1.75	10	0	0	0
BC-SBR	100	2	2	0.5	3	1.75	0	10	0	0
SI-CS-PVA-SBR	100	2	2	0.5	3	1.75	0	0	10	0
BC-CS-PVA-SBR	100	2	2	0.5	3	1.75	0	0	0	10

^a*N*-Cyclohexyl-2-benzothiazole-sulfonamide. ^b2,2-Dibenzothiazolyl disulfide. ^cphr, part per hundreds of rubber.

Table 2. Curing Characteristic Results

	Maximum torque, M_H (dNm)	Minimum torque, M_L (dNm)	ΔM (dNm)	Scorch time, t_{s2} (min)	Cure time, t_{90} (min)	Cure rate index, CRI (min ⁻¹)
Neat SBR	9.44	3.59	5.85	6:30	13:05	15.77
SI-SBR	22.12	7.72	14.40	7:45	15:27	12.90
BC-SBR	22.93	6.47	16.46	6:47	10:55	24.10
SI-CS-PVA-SBR	27.50	7.69	19.81	1:46	3:34	55.56
BC-CS-PVA-SBR	30.04	6.46	23.58	2:16	4:00	57.80

two methods applied for the investigation of viscoelasticity: Strain sweep and frequency sweep. Strain sweep was hold on at 60 °C from 0.05° to 20°, with the frequency fixed at 60 cpm (circle per minute). Frequency sweep was hold on from 1 to 120 cpm, at the temperature of 60 °C and at the strain amplitude of 1°. Characteristics related to viscoelasticity of composites could be obtained, which varied with the strain amplitude or the frequency.

Results and Discussion

Curing test results of compounds with additives were displayed in Table 2. The torque values of all the samples had been increased, due to the strength of fillers, which strongly restricted the deformation and consequently increased the mechanical properties of SBR composites. The curing rate index (CRI) was applied to indicate the vulcanization rate. The CRI values of SI-SBR was decreased compare to the neat SBR, because when SBR compounded with SI powder, the filler aggregation affected chain mobility,¹¹ which will reduce the vulcanization rate. But as compounds filled with SI-CS-PVA hybrid filler and BC-CS-PVA hybrid filler, because the more compact interpenetrating crosslinking structure between rubber and gel-BC/SI hybrid had been formed, the dislocation

effect may not reduce the chain mobility due to the adsorption effect of gel hybrid, which would short the distance of rubber chains. Thus, the CRI of compounds filled with hybrid fillers has larger values than neat SBR compound. Also, the compounds filled with gel hybrids had larger M_H and ΔM than neat SBR, due to the effect of adsorption and IPN structure with physical crosslinking, which can make the matrix structure more compact and stable.¹² From this table, it can be found the M_H , ΔM and the CRI value of BC-CS-PVA-SBR are the largest, which means this composite may have the best mechanical and viscoelastic properties. The possible reason of this phenomenon is: The adsorption force¹³ of interpenetrating gel structure would short the distance of rubber chains, which would form the more compact matrix. So the curing rate of hybrids filled compounds will be faster than other compounds include the neat SBR.

Dynamic strain amplitude sweep tests of neat SBR, SI-SBR, BC-SBR, SI-CS-PVA-SBR and BC-CS-PVA-SBR were tested by an RPA. The network structure and the internal interactions in the composites before the curing were analyzed under dynamic deformation. The dependence of storage modulus (G'), loss modulus (G''), elastic torque (S') and viscos torque (S'') on strain amplitude is exhibited in Figure 4 and Figure 5.

At the initial step of the strain sweep, the magnitudes of G'

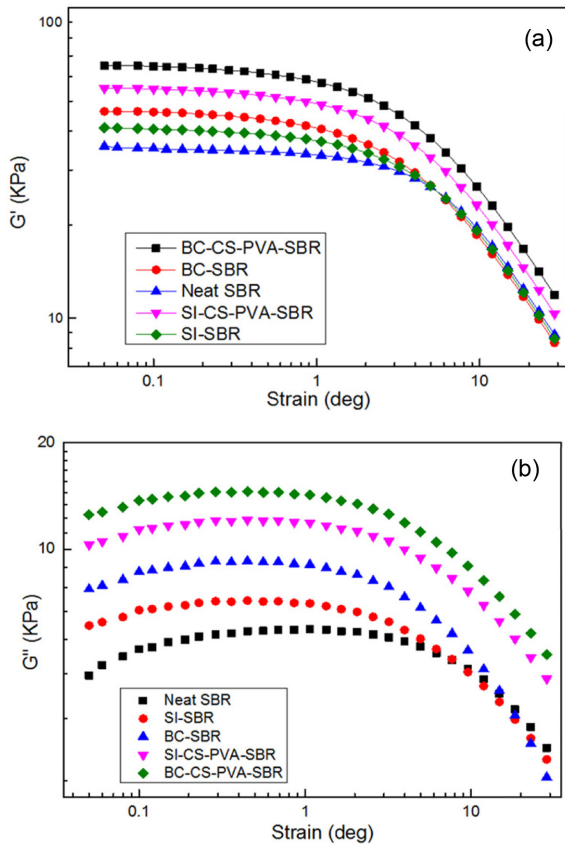


Figure 4. Dynamic strain sweep of (a) G' ; (b) G'' for composites at a frequency of 60 cpm and at a temperature of 60 °C.

of all the samples showed a linear plateau region as the strain amplitude was lower than 5°. But with the strain value increasing, the values of G' deviated from the linear region and rapidly decreased to lower than 15 KPa. The probably reasons are the breakup of the filler-filler network¹⁴ and the destruction of the filler-polymer interactions.¹⁵ And the other important reason is the disentanglement of the IPN with the strain increased, which would show the decreasing of G' .

The loss modulus (G'') of composites is commonly related to energy dissipation during deforming, which is associated with the breakage¹⁶ and reformation of filler-filler network and slippage of the polymer chains.

From the curves in the Figure 4(b), it can be found at the initial step of the strain sweep, the magnitudes of G'' were increased, with the strain amplitude over 5°, the values of all the sample decreased rapidly due to the low temperature cannot make samples to be completely vulcanized, so the weak filler-polymer interactions and the motion of the uncrosslinking rubber chains might be reasons of that phenomenon.¹⁷ All the G'' values were lower than the corresponding values of

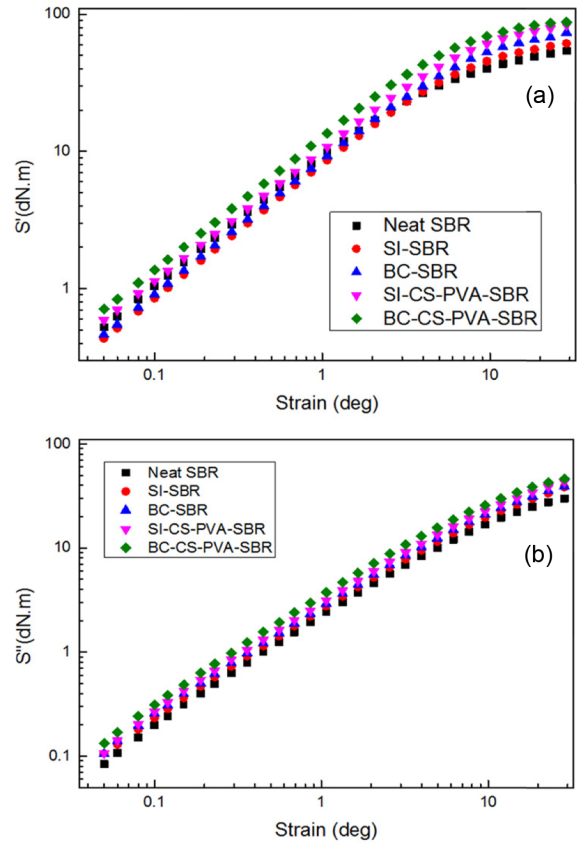


Figure 5. Dynamic strain sweep of (a) S' ; (b) S'' for composites at a frequency of 60 cpm and at a temperature of 60 °C.

G' , which means all the samples have solid-like behavior ($\tan \delta < 1$).¹⁸

In Figure 4, the curves of SI/BC-CS-PVA-SBR always are on the top, especially the BC-CS-PVA-SBR showed the largest values, which means BC-CS-PVA-SBR has the largest storage modulus and loss modulus in this research.

With the bilogarithmic coordinates, S' and S'' always showed almost linearly dependent on strain (shown in Figure 5). But at high strain (>10°), the sulfur crosslinks and the filler-filler interactions ruptured which led to a descending slope.¹⁹ Dynamic frequency sweep tests were conducted in the linear viscoelastic region for further study on network formation and microstructural changes of the composites in detail.²⁰ The logarithmic plot of G' and η^* versus angular frequency resulting from the dynamic frequency scan measurements at 60 °C of all the samples was shown in Figure 6, respectively, the low frequency region of the rheological plot reflects the effect of structure of IPN on the viscoelastic properties of the composites.²¹ Therefore, to find the interactions of SI/BC-CS-PVA hybrid fillers on the rheological behavior of the composites,

the dependence of modulus and η^* on the frequency was studied at low frequencies (120 cpm).

All the samples' data showed in Figure 6(a), G' was almost linearly dependent on frequency. At low frequency region, the G' range was higher, they narrowed down at high frequency stage. The reason is at low frequency, there is enough time for unraveling of the entanglements leading to a large amount of relaxation,²² resulting in a low value of G' . But when a rubber matrix is deformed at higher frequency the entanglement chains have no time to relax, so the modulus increases. The strong interaction forces via hydrogen bonding between SBR rubber matrix and hybrid fillers, which could cause the increasing of G' .

It is observed from Figure 6(b) than the complex viscosity (η^*) decreased with the increasing in frequency. This is due to the strong shear thinning behavior of the polymer composites and their pure equivalent with the lower shearing rate.²³ The dynamic viscosity of SI/BC-CS-PVA-SBR in the high frequency region is appreciably higher compared to that of pure SBR, which means IPN structure contributed to the increase of

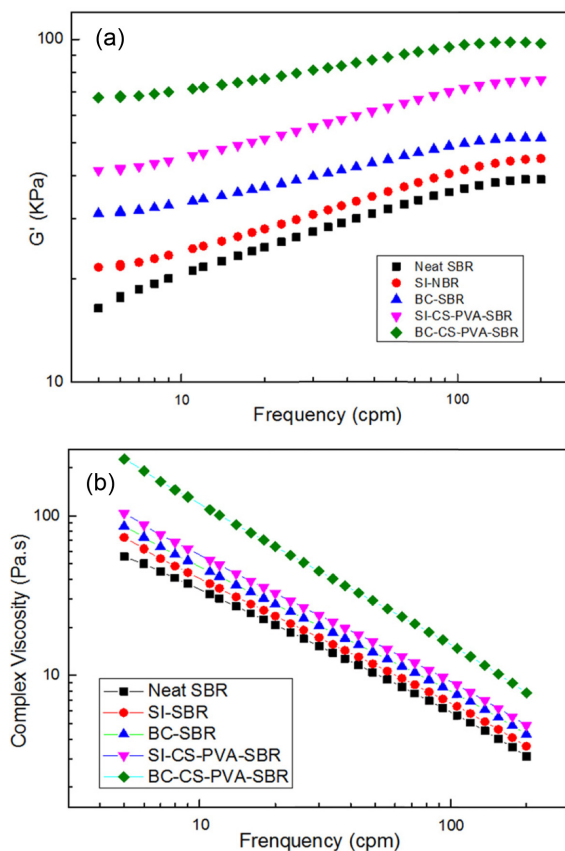


Figure 6. Dynamic strain sweep of (a) G' ; (b) η^* for composites at a strain of 1° and at a temperature of 60°C .

complex viscosity of SBR matrix, which hindered the molecular slippage during shearing.²⁴

Cole-Cole plots²⁵ are shown in Figure 7, which describe the relationship between complex viscosity (η^*) and real viscosity (η'). It describes the structure of heterogeneous materials, such as the samples in this work. Obviously, all the composites showed Cole-Cole plots in linear shape, which means the solid like viscoelastic response. And with the incorporation of fillers, the Cole-Cole plots were more linear than the neat SBR.

The reason is when the fillers dispersed in the matrix, it would affect the relaxation process during frequency sweep by forming a filler-rubber network.²⁶ And SI/BC-CS-PVA-SBR showed the best linear shape compared with others, which means they could indicate stronger interpenetrating filler network formed in SBR matrix.

Loss factors $\tan \delta$ of all the samples as a function of strain were presented in Figure 8. From this figure, it can be found at low strain (<1 degree), the order of $\tan \delta$ is neat SBR $>$ BC-SBR $>$ SI-SBR $>$ SI-CS-PVA-SBR $>$ BC-CS-PVA-SBR, whereas at high strains (>1 degree), this trend completely reversed. It is due to different modes of energy dissipation at low & high strain regions.²⁷ At low strain, matrix structure was almost not destroyed, and the viscos nature of rubber would mainly be responsible for the energy dissipation.²⁸ Due to no restriction of filler, neat SBR exhibited the highest $\tan \delta$, and BC-CS-PVA-SBR showed the lowest $\tan \delta$, which may be interpreted in terms of reduction in deformable rubber fraction. At high strain, the matrix structure was gradually destroyed, and the hysteresis was almost from filler-filler friction due to the destruction of filler agglomerations.²⁹ And the interfacial friction between filler and matrix, the viscos characteristic of rubber fraction released from within filler agglomerations also

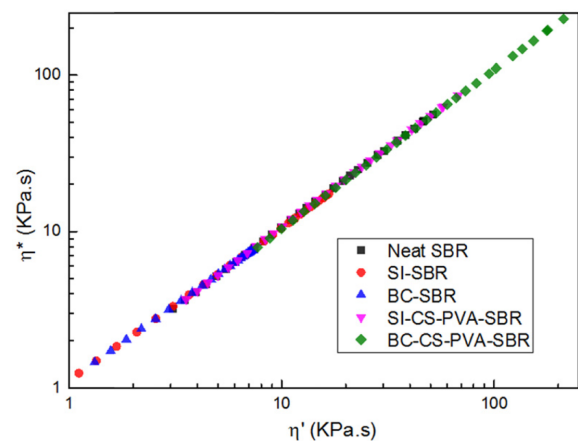


Figure 7. Cole-Cole plots of η^* versus η' .

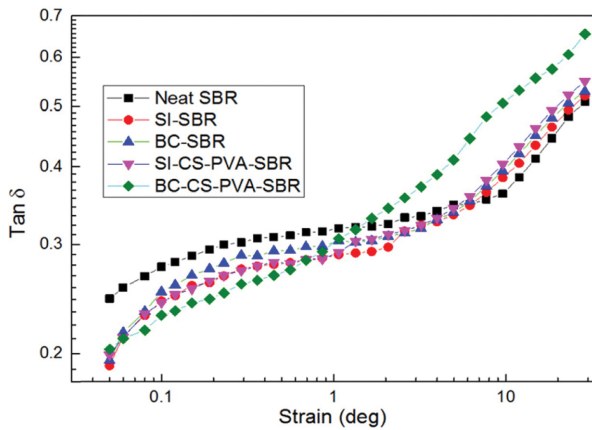


Figure 8. $\tan \delta$ for composites from dynamic strain sweep at a frequency of 60 cpm and at a temperature of 60 °C.

contributed to the hysteresis.³⁰ As BC-CS-PVA-SBR, the breakdown of filler agglomerations increased filler-filler friction, and in the meantime the weaker interfacial interaction also increased the interfacial friction between filler and matrix.³¹ So BC-CS-PVA-SBR exhibited the highest $\tan \delta$ in high strain region.

Figure 9 shows the SEM graphs of the fracture surface for (a) CS-PVA gel, (b) neat SBR, (c) SI-SBR, (d) BC-SBR, (e) SI-CS-PVA-SBR, and (f) BC-CS-PVA-SBR, all the rubber sample matrixes were characterized after the tensile test, respectively. As can be seen from the graphs, the fracture surface of CS-PVA gel was shown in Figure 9(a), it can be found a smooth and complete surface, which meant the gel has compact structure. And Figure 9(b) is for the neat SBR, compared to Figure 2(b)~2(f) showed the difference between the neat SBR and composites filled with fillers. From Figure 9(c) and 9(d), it can be found more gully-like structure in BC-SBR than SI-SBR, which meant better compatibility with SBR latex. And from Figure 9(e) and 9(f), it can be found so much gully-like structure in the pictures, which also meant the interpenetrating network structure was formed into these two composites, and due to the agglomeration effect, SI showed the larger blocks state and larger porous structure into the hybrid system after the tensile strength test. But BC blocks looked smaller obviously, which meant BC had better combination effect with the CS-PVA gel system. And due to the hydrophilic properties, BC showed less hydrophilicity compared to the SI, so when fixed with SBR latex, which could improve the interpenetrating network. It also contributed to the most compact structure of matrix, which could provide the best mechanical properties for the SBR latex composites after filling process.

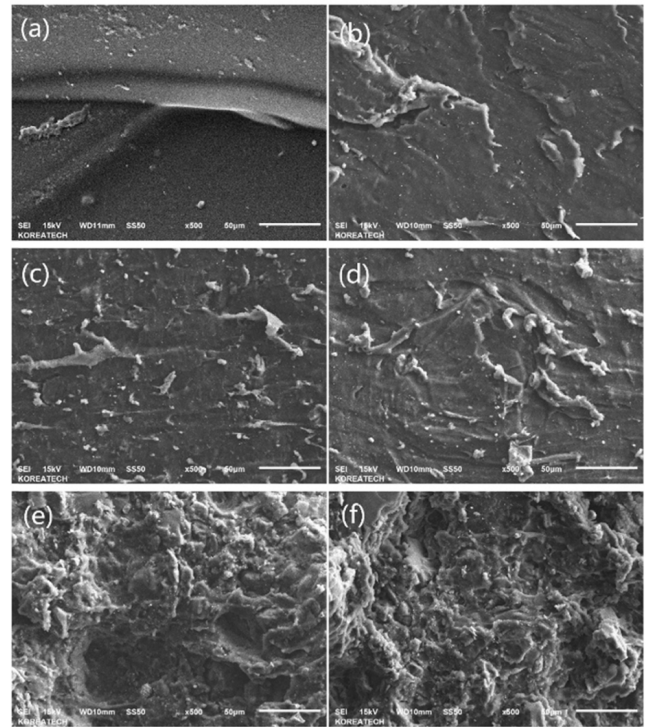


Figure 9. SEM images for (a) CS-PVA gel; (b) neat SBR; (c) SI-SBR; (d) BC-SBR; (e) SI-CS-PVA-SBR; (f) BC-CS-PVA-SBR.

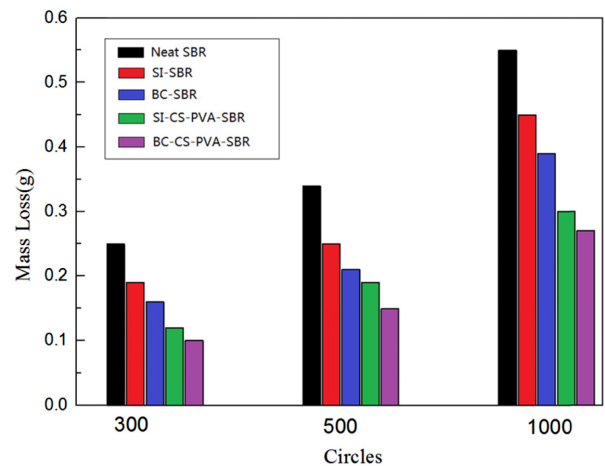


Figure 10. Abrasion resistance results of composites.

The results of abrasion resistance were shown in Figure 10, from this figure, it can be found the mass loss decreased after filling process, which means these compounds' abrasion resistance were improved, and the BC-CS-PVA-SBR showed the best resistance reinforcement effect. The probably reason is due the most interpenetrating crosslinking structure, it can improve high hardness value of matrix, and make matrix more compact, which also influence the abrasion resistance.

Conclusions

In this work, the chitosan-PVA-bamboo charcoal/silica (BC/SI-CS-PVA) hybrid fillers compatibilized styrene-butadiene rubber composites were successfully prepared by interpenetrating polymer network (IPN) method. In this way, the compact interpenetrating polymer network had been formed which caused the highest G' , G'' , S' and S'' of the BC-CS-PVA-SBR composites from the results of strain sweep. It means this hybrid filler could provide best mechanical and viscoelastic reinforcing effect. And from the results of frequency sweep, BC-CS-PVA-SBR also showed the best storage modulus (G') and complex viscosity value, which also means BC-CS-PVA filler could contribute to viscoelastic behaviors of the SBR rubber materials. From the result of Cole-Cole plots curves, it can be found that BC-CS-PVA showed the best solid-like viscoelastic response, it means that BC-CS-PVA could indicate stronger interpenetrating filler network formed in SBR matrix. Also, the results in the SEM graphs exhibited the fracture surface of CS-PVA gel and all the rubber samples in this research, which could find BC-CS-PVA-SBR has the most compact matrix structure. The results of abrasion resistance also showed BC-CS-PVA-SBR could provide the best abrasion resistance.

References

1. E. C. Larsen and J. H. Walton, *J. Phys. Chem. A*, **44**, 70 (1940).
2. X. X. Li, X. Ge, and U. R. Cho, *Polym. Korea*, **40**, 933 (2016).
3. W. Nitayaphat, N. Jiratumnukul, S. Charuchinda, and S. Kittinaovarat, *Carbohydr. Polym.*, **78**, 444 (2009).
4. X. X. Li, J. H. Oh, S. H. Kang, S. H. Jang, D. H. Lee, and U. R. Cho, *Polym. Korea*, **41**, 750 (2017).
5. J. W. Lee, S. Y. Kim, S. S. Kim, Y. M. Lee, K. H. Lee, and S. J. Kim, *J. Appl. Polym. Sci.*, **73**, 113 (1999).
6. D. Schmaljohann, *Adv. Drug Delivery Rev.*, **58**, 1655 (2006).
7. P. Matricardi, C. D. Meo, T. Coviello, W. E. Hennink, and F. Alhaique, *Adv. Drug Delivery Rev.*, **65**, 1172 (2013).
8. T. Ando and J. Skolnick, *Proc. Natl. Acad. Sci. USA*, **107**, 18457 (2010).
9. X. X. Li and U. R. Cho, *Polym. Korea*, **42**, 1 (2018).
10. K. K. Rao, B. V. K. Naidu, M. C. S. Subha, M. Sairam, and T. M. Aminabhavi, *Carbohydr. Polym.*, **66**, 333 (2006).
11. M. S. Sobhy, D. E. El-Nashar, and N. A. Maziad, *Egypt. J. Sol.*, **26**, 241 (2003).
12. X. Ge, M. C. Li, and U. R. Cho, *Polym. Compos.*, **36**, 1063 (2015).
13. D. H. Jung, D. J. Kim, T. B. Lee, S. B. Choi, J. H. Yoon, J. H. Kim, K. H. Choi, and S. H. Choi, *J. Phys. Chem. B*, **110**, 22987 (2006).
14. G. A. Bohm, W. Tomaszewski, W. Cole, and T. Hogan, *Polym.*, **51**, 2057 (2010).
15. J. Jancer, J. F. Douglas, F. W. Starr, S. K. Kumar, P. Cassagnau, A. J. Lesser, S. S. Sternsteinh, and M. J. Buehler, *Polym.*, **51**, 3321 (2010).
16. Y. K. Chen, Y. P. Wang, and C. H. Xu, *J. Macromol. Sci. B*, **51**, 1921 (2012).
17. M. J. Wang, *Rubber Chem. Technol.*, **71**, 520 (1998).
18. G. Dimitreli and A. S. Thomareis, *J. Food. Eng.*, **84**, 368 (2008).
19. X. Ge, Z. Zhang, H. Yu, B. Zhang, and U. R. Cho, *Appl. Clay Sci.*, **157**, 274 (2018).
20. A. Durmus, A. Kasgoz, and C. W. Macosko, *Polym.*, **48**, 4492 (2007).
21. X. Hu, J. Fan, and C. Y. Yue, *J. Appl. Polym. Sci.*, **80**, 2437 (2001).
22. K. Wang, Y. Chen, and Y. Zhang, *Polym.*, **49**, 3301 (2008).
23. R. Krishnamoorti and K. Yurekli, *Curr. Opin. Colloid Interface Sci.*, **6**, 464 (2001).
24. S. Gan, Z. L. Wu, H. Xu, Y. Song, and Q. Zheng, *Macromolecules*, **49**, 1454 (2016).
25. K. S. Cole and R. H. Cole, *J. Chem. Phys.*, **9**, 341 (1941).
26. J. Leopoldes, C. Barres, J. L. Leblanc, and P. Georget, *J. Appl. Polym. Sci.*, **91**, 577 (2004).
27. R. E. Shadwick, *J. Appl. Physiol.*, **68**, 1033 (1990).
28. M. J. Wang, *Rubber Chem. Technol.*, **71**, 520 (1998).
29. Z. Li, W. Ren, H. Chen, L. Ye, and Y. Zhang, *Polym. Int.*, **61**, 531 (2012).
30. M. Luo, X. Liao, S. Liao, and Y. Zhao, *J. Polym. Sci.*, **129**, 2313 (2013).
31. J. Jordan, K. I. Jacob, R. Tannenbaum, M. A. Sharaf, and I. Jasiuk, *Mat. Sci. Eng. A-Struct.*, **393**, 1 (2005).